PHYSICAL REVIEW C VOLUME 21, NUMBER 6 JUNE 1980

Scattering and reaction dynamics for the $^{12}C+p$ system

J. R. Comfort and B. C. Karp
Department of Physics and Astronomy, University of Pittsburgh, Pittsburgh, Pennsylvania 15260
(Received 1 October 1979)

Elastic scattering data for proton scattering from ^{12}C are analyzed phenomenologically by use of local, complex, one-channel optical-model potentials and in an extended coupled-reaction-channel environment. Although the back-coupling amplitudes in the elastic channel from pickup-stripping paths through ^{11}C intermediate states are found to be quite sizable, the optical-model potential is able to simulate most of the effects quite well for both scattering and reaction processes at energies greater than about 60 MeV. The parameters of the optical-model potential and the residual optical-model potential of the coupled-reaction-channel environment are found to vary smoothly with energy. Below 60 MeV, these parameters have quite different trends and the ability of the one-channel optical-model potential to simulate the singular effects of strong couplings is much reduced.

[NUCLEAR REACTIONS $^{12}C+p$ system, energies up to 185 MeV; optical-model phenomenological analysis; coupled-reaction-channel analysis; comparison with DWBA calculations.]

I. INTRODUCTION

The recent extension of high-quality nuclear reaction experiments to intermediate energies raises many issues regarding the reaction mechanisms. For convenience it is hoped that many of the tools and techniques developed for low-energy applications, such as local, phenomenological, optical-model potentials (OMP), partial-wave expansions, and coordinate-space representations, might be readily extended to the higher energies. Conversely, one might also hope that certain difficulties such as exchange contributions and coupled-channels effects might be reduced so that the data will be more sensitive to the nuclear-structure information inherent in reaction processes at higher momentum transfers. Since it is known, for example, that deuteron D-state contributions for (p,d) or (d,p) reactions are beginning to become important at these energies,[1] the hopes can never be fully realized. Careful studies of the significant ingredients to the reaction dynamics are therefore required.

Reactions on ^{12}C can provide an excellent opportunity for such studies. The number of states in this nucleus and its neighbors is small enough to make many calculations feasible and much information is available about the wave functions. The extensive and very satisfying analysis of 122-MeV (p,p') data from ^{12}C and ^{14}N in the preceding article[2] illustrates quite well the possibilities that are available here. Indeed, the present article arose out of the need for a reliable treatment of the reaction dynamics in that analysis of effective interactions.

It has often been argued, of course, that the large permanent deformation of ^{12}C and the consequent strong couplings to excited states in inelastic scattering processes makes reaction analyses unreliable. We find, however, that these couplings are by far not the most important ones. Yet, as the energy increases, the disturbing effects of all the couplings decrease and, at intermediate energies, ^{12}C is as tractable for study as other nuclei.

At issue here is the ability of the local, one-channel, phenomenological OMP to represent the implicit effects of couplings between the elastic and reaction channels on scattering and reaction cross sections. This, of course, is the principal role of the imaginary part of the complex OMP, although the real part must make some contributions as well.[3,4] An understanding of this role will enhance our knowledge of the OMP itself, particularly with respect to its microscopic foundations. It should also enhance our confidence in calculations of reaction dynamics and in the inferences of nuclear properties based on parametrizations of empirical potentials.

Remarkable progress has been made recently[5,6] on the microscopic foundations of the OMP and this has elucidated many of the features of the phenomenological potentials. In these works both the real and imaginary parts arise naturally from the construction of the complex two-nucleon t matrix (or G matrix) in nuclear matter. This *a priori* approach has been unusually successful in reproducing elastic scattering data, but the relationship of the OMP so constructed to channel couplings is not at all transparent.

An alternative approach, particularly for the

imaginary part, might be the direct calculation of the ingredients of the OMP from a realistic treatment of reaction processes.[7] This would involve specific assumptions regarding the detailed structure of the nucleus of interest and its neighbors, as well as a thorough calculation of the reaction dynamics, possibly with an exact solution of the coupled equations. Since the channel space must necessarily be truncated, the remaining OMP must still be adjusted to fit empirical data and will remain complex. We shall refer to this as a residual OMP (ROMP). It is defined for use in an extended mutichannel environment.

A one-channel OMP might be said to be equivalent to a ROMP (each with its appropriate environment) if they reproduce elastic scattering data equally well. The use of one-channel OMP's in distorted-wave Born-approximation (DWBA) calculations of particular reactions is an extension of this equivalence and the general success of this approach provides support for it. Nevertheless, it is entirely possible that, due to their strengths, certain individual channel couplings may have a singular influence on elastic scattering and/or reaction cross sections and that this cannot be simulated reliably by an average local OMP. The frequent use of multistep and coupled-channel (CC) calculations for reactions attests to these singular influences in many instances.

It is not easy to obtain information on such questions. Mackintosh has made extensive studies on heavier nuclei and at energies below 50 MeV.[3,4,8] He has considered environments in which the elastic channel is strongly coupled to both inelastic scattering and pickup channels. Valuable insights have come from the demand that the ROMP's give the same elastic scattering as a conventional OMP. The present article is similar in approach. Although much of the work was developed independently, and benefited from the use of automatic search procedures,[9] many of the general conclusions are the same.

The present work is devoted to an intensive and systematic study of the dynamics of proton induced reactions on ^{12}C at intermediate energies. Elastic scattering data are taken from the literature for energies up to 185 MeV, with the primary emphasis in the range 60–185 MeV. Although there are considerable data at lower energies, they have been given little attention here. The concern is mainly for intermediate energies. As will become clear in Secs. IV and V, numerous difficulties are also encountered in the lower range.

After a conventional analysis in terms of the conventional one-channel optical model (OM), attention is given to a vigorous treatment of a coupled-channel environment within the framework of a specific model. The scattering data are refitted in this environment. Conclusions may be reached regarding the energy dependence of the parameters of the OMP and ROMP as well as for the specific importance of the coupled channels. Reports on portions of this work have already been given.[10–12]

II. DATA SELECTION

A. General considerations

Examination of the literature reveals that data for proton scattering from ^{12}C are available at a number of energies between 60 and 185 MeV, but are of diverse vintage and quality. Our interest was not in making a global analysis of all the data, but rather in more detailed studies at selected energies spread smoothly across the range. Preliminary inspections suggested that the best data were available near 60, 120, and 180 MeV. Data at some values more closely spaced were also desired.

In the literature it is not always unambiguously clear whether the data are presented in laboratory or center-of-mass frames and, if the latter, whether relativistic or nonrelativistic kinematics were used for the conversion. The questions could usually be resolved by detailed numerical inspection. We adopted the policy of tabulating absolute center-of-mass cross sections with nonrelativistic kinematics used for the conversion for energies below 80 MeV, and relativistic kinematics above 80 MeV. This corresponds to common historical practice, but necessitated adjustments of some of the data sets.

In order to gauge the reliability of the available data, the absolute cross sections for the various data sets were plotted against momentum transfer q. The data thought to be the most reliable then revealed a systematic pattern, particularly in the range $50 \leq q \leq 150$ MeV/c. (For orientation, the first maximum in the ratio-to-Rutherford cross section occurs at $q = 155 \pm 5$ MeV/c for all energies above 40 MeV). This pattern allowed judgments to be formed about the other data, as will be indicated in Sec. II B.

Since studies of optical-model parameters normally benefit from polarization data, an effort was made to find energies where both cross-section and polarization data existed. There have been few polarization measurements at intermediate energies and they are often at energies where the differential cross sections seem less reliable. Since the search program[9] required identical energies for simultaneous fitting, the polarization data at some energies were used for

other energies by changing the angle scale according to the relation $\theta\sqrt{E}$ = constant. Test calculations indicated that this assumption was reasonable for the individual cases. In practice, the polarization data were not a strong constraint on the results of the search procedures.

Since the model space for the CC calculations included inelastic scattering and pickup channels, data for (p,p') and (p,d) reactions on ^{12}C were also obtained whenever possible. Tabulations were often not available, but the cross sections could be read from graphs with sufficient accuracy.

Apart from the above considerations, the data were taken as given in the literature. In particular, no adjustments were made to the errors so as to take into account the uncertainties in scattering angles. Absolute values for the goodness-of-fit parameter χ^2 may therefore not have much significance. The emphasis of the present study is on systematic trends. At each energy an effort was made to minimize χ^2.

B. Individual choices

Although our principal interest was in energies above 60 MeV, a partial study was also made at 40 MeV. Following is a brief discussion of the data and adjustments made to them.

1. 12.07 and 21.65 MeV

Since the CC analyses also required proton OMP's at substantially lower energies, data for 12.07 and 21.65 MeV were selected specifically for this purpose. The systematic study of differential cross sections by Nagahara[13] was used for 12.07 MeV. Cross sections have been measured at 21.6 MeV (Ref. 14) and polarizations at 21.7 MeV.[15]

2. 40.0 MeV

Both differential cross sections and polarizations have been measured by Blumberg *et al.* for several nuclei at 40 MeV.[16] The data are closely spaced and extend over the full angular range.

3. 61.4 MeV

Elastic scattering cross sections out to about 110° have been reported by Fulmer *et al.* at 61.4 MeV.[17] Although polarization data were not available, (d,p) data have been published for 65 MeV.[18]

4. 96 MeV

Cross-section data at 96 MeV (Ref. 19) are mainly concentrated at angles $\leq 30°$, but numerous data points extend to almost 90°. Nonrelativistic kinematics had originally been used for the center-of-mass tabulation,[19] which was also given in ratio to the Rutherford cross section. Comparisons with the 95-MeV data of Dickson and Salter[20] indicate that their cross sections are consistently low by about 15%. Data at 100 MeV[21] are untabulated. Neither set of data was used.

5. 122 MeV

Differential cross sections for elastic scattering were reported in Ref. 2. Polarization angular distributions are in the process of being measured[22] and the data of Dickson and Salter[20] for 135-MeV protons were extrapolated to this energy. Measurements of the (p,d) and (p,p') cross sections are also available.[2,23]

6. 135 MeV

The systematic trends of the q-space plots suggested that the 135-MeV differential cross sections of Dickson and Salter[20] were low by 15–20%, as was also the case for their 95-MeV data. This exceeds their quoted uncertainty of 7%. Since the angles were tabulated for the laboratory reference frame, it was assumed that the cross sections were also, although the Jacobian for the center-of-mass transformation could account for the discrepancy. When multiplied by 1.15, the cross sections gave good agreement with systematic trends. Since the polarization data seemed valuable to have, the data were used in this modified form.

7. 144 MeV

Very accurate differential cross sections are available for $\theta < 20°$ at 144 MeV.[24] Data also exist for $\theta > 20°$ at 145 MeV,[25] but the errors are substantial and the cross sections do not extrapolate smoothly from the 144-MeV results. Since the 145-MeV data extend to quite large angles, and polarization measurements were also reported,[25] it is unfortunate that they could not be used for more than a qualitative check on the systematics.

8. 150–156 MeV

The systematics of the q-space plots indicate clearly that the 150-MeV differential cross sections of Rolland *et al.*[26] are low by up to 20%, depending on the angle. The measurements of Comparat *et al.*[27] at 156 MeV are untabulated. Again the inability to use the cross sections is regretted since polarization data are available at these energies.[26,28]

9. 183 MeV

Excellent data for elastic scattering cross sections are available at 183 MeV, with a few extra

data points for large angles at 177 MeV.[29] A companion paper[30] gives data for total reaction cross sections at the same energy and has a useful graph of their energy dependence. Polarization data were extrapolated from 155 MeV (Ref. 28) since the very recent data at 185 MeV (Ref. 31) were not available at the time of this study. There is very little difference with the extrapolated data. Data for the (p,p') reaction[32] and the (p,d) reaction,[33] both at 185 MeV, are also available.

III. OPTICAL-MODEL ANALYSIS

In this section we consider a conventional analysis in terms of the one-channel optical model. Attention is directed to systematic trends.

A. Optical model

Representing the scattering wave function by a partial-wave expansion in the usual manner, the radial Schrödinger equation to be integrated is

$$\frac{d^2\chi_{lj}(r)}{dr^2}+\left[k^2-\frac{2\mu}{\hbar^2}U(r)-\frac{l(l+1)}{r^2}\right]\chi_{lj}(r)=0\,. \quad (1)$$

$U(r)$ is the local optical potential

$$U(r)=V_c(r)+Vf(r)+iWf'(r)+iW'a\frac{d}{dr}f'(r)$$
$$+\frac{1}{r}\left[V_{so}\frac{d}{dr}f_{so}(r)+iW_{so}\frac{d}{dr}f_{so}(r)\right]\vec{l}\cdot\vec{s}\,. \quad (2)$$

The Coulomb potential

$$V_c(r)=\begin{cases}\dfrac{\eta k}{R_c}(3-r^2/R_c^2) & \text{for } r<R_c\,,\\ 2\eta k/r & \text{for } r\geq R_c\end{cases} \quad (3)$$

corresponds to a uniformly charged sphere, with $R_c=r_cA^{1/3}$. The complex nuclear potential may contain volume Woods-Saxon potentials of strengths V and W and with radial shapes

$$f(r)=1/(1+e^x)\,,\quad x=(r-R)/a\,,\quad R=r_0A^{1/3}\,, \quad (4a)$$

$$f'(r)=1/(1+e^{x'})\,,\quad x'=(r-R')/a'\,,\quad R'=r'A^{1/3}\,. \quad (4b)$$

Optionally, the imaginary part may have a surface term with strength W' and radial dependence $-e^{x'}/(1+e^{x'})^2$. The radial form $f_{so}(r)$ of the spin-orbit potentials is the same as in Eq. (4) and the usual $(\hbar/m_\pi c)^2$ factor is included in the strengths.

In the automatic parameter search procedures, the program CUPID[9] attempts to minimize χ^2, the measure of goodness of fit defined by

$$\chi^2=\sum_{i=1}^{N}\left(\frac{y_i^{\rm exp}-y_i^{\rm th}}{\Delta y_i^{\rm exp}}\right)^2, \quad (5)$$

where $y_i^{\rm exp}$ is the experimental value with error $\Delta y_i^{\rm exp}$ and $y_i^{\rm th}$ is the theoretical value. These may be differential cross sections or polarizations. It is common to report χ^2/N separately for these quantities.

B. Kinematics

As projectile energies increase, relativistic effects become more important. For convenience the nonrelativistic Schrödinger equation may still be used, but it is common to calculate the kinematic quantities k, μ, and η with relativistic expressions.

Convenient relationships are easily found.[34] We let a projectile of mass m and with kinetic energy E be incident on a target with mass M and set $\hbar=c=1$. The total energy of the system is

$$T=[(m+M)^2+2ME]^{1/2} \quad (6)$$

and the center-of-mass wave number is

$$k=(E^2+2Em)^{1/2}M/T\,. \quad (7)$$

The total energies of the particles in the center-of-mass frame are

$$w=(m^2+mM+ME)/T\,, \quad (8a)$$

and

$$W=(M^2+mM+ME)/T\,. \quad (8b)$$

The reduced mass μ is appropriately replaced with the reduced energy

$$\mu=wW/(w+W)\,. \quad (9)$$

Finally, for both forms of the kinematics, the Coulomb parameter is

$$\eta=zZe^2\mu/k\,, \quad (10)$$

where z and Z are the charges of the colliding nuclei and μ has units of energy.

Since the Coulomb cross section is proportional to $(\eta/k)^2$, among other factors, the choice of kinematics affects the ratio-to-Rutherford values. It also affects the conversion between laboratory and center-of-mass frames. Relativistic kinematics were used for all energies above 80 MeV.

One should note that the potentials extracted from the data are defined with respect to the chosen kinematics. They should not be used with the other choice. There are no extra factors and the approximations of a commonly used alternative[35] are avoided.

C. Search procedures

Parameter studies were carried out for each energy separately. These included numerous

calculations with different starting values, varying choices of the parameters to be searched, and some calculations with constraints between parameter pairs. When trends and systematic features were noted, these were then adopted and searches were made with fewer parameters. Thus, the final results partly reflect the systematic features and partly the individual characteristics.

Early efforts were devoted to eliminating unnecessary parameters. In order to avoid family ambiguities, the radius of the real potential was fixed at $r_0 = 1.20$ fm (except at 12.07 MeV). This seemed to be the best value at 21 MeV and the data at all higher energies were not very sensitive to it, although some improvements in χ^2 could sometimes be obtained with a slight increase.

Volume absorption seemed reasonable and acceptable at all energies. At 21 MeV, pure surface absorption gave inferior results and mixed surface and volume forms were no improvement over pure volume absorption. Systematic parametrizations for heavier nuclei indicate that volume absorption should dominate at higher energies and be negligible near 12 MeV.[36] For this reason pure surface absorption was used only for the 12.07 MeV data.

The spin-orbit potentials were particularly interesting. All the data above 60 MeV required significantly smaller values of the geometrical parameters than those at lower energies. The χ^2 minima in parameter space were exceedingly narrow and changes of 0.01–0.02 fm in r_{so} or a_{so} could have quite deleterious effects. Some studies were also made of the imaginary spin-orbit potential. The data seemed not to be very sensitive to it. Searches begun with either sign of W_{so} usually terminated with the same sign or near zero with little improvement in the final χ^2. Hence we have taken $W_{so} = 0$ in all cases.

D. Results

The final OM fits to the differential cross sections are shown by solid curves in Figs. 1–5 and for polarizations in Figs. 6 and 7. Figure 8 presents the volume integrals per nucleon for the real, imaginary, and spin-orbit parts of the potential. The geometrical parameters are plotted as solid lines in Fig. 9. Values are listed in Table I.

It is apparent from the trends in Figs. 8 and 9 that the parametrization seems smooth at energies above 60 MeV, but is irregular below that. This is our first indication of a qualitative difference in the scattering of protons from ^{12}C

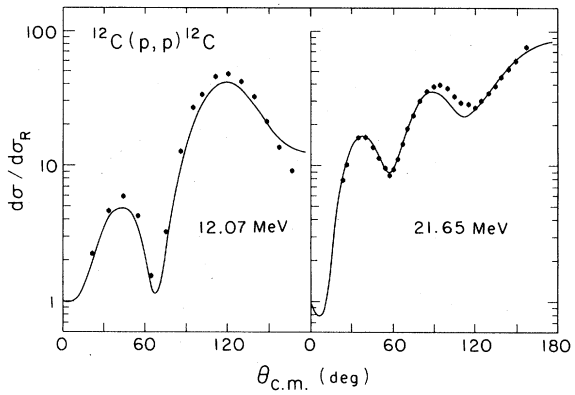

FIG. 1. One-channel optical-model calculations for proton elastic scattering from ^{12}C, in ratio to the Rutherford cross sections.

above and below 60 MeV. We may discuss individual features in these regions separately.

1. $E < 60$ MeV

The fit to the 12.07-MeV data in Fig. 1 is good. It is a little worse than in a previous analysis,[37] due mainly to our desire to keep the diffuseness parameters from becoming too small. Okai and Tamura showed[38] that broad resonances brought about by the couplings to other channels might be present in this energy range. It is possible that the unusual parameters at this energy are reflecting these couplings.

Although resonances have been alleged to play an important role near 20–25 MeV,[39] our pure OM results in Figs. 1 and 6 with reasonable parameters are superior to other parametrizations.[15,34,40]

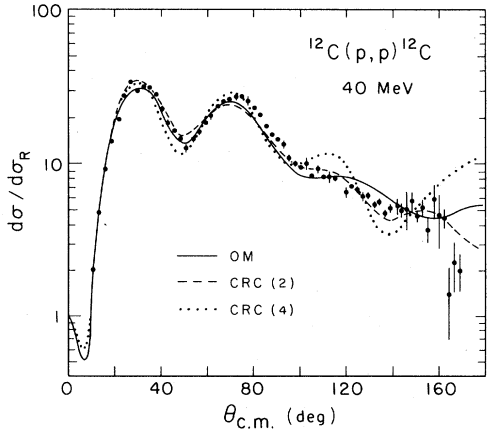

FIG. 2. Proton elastic scattering from ^{12}C in ratio to the Rutherford cross sections. The solid curve is a pure optical-model calculation. The dash and dotted curves result from CRC calculations after two and four iterations, respectively, of the search procedures.

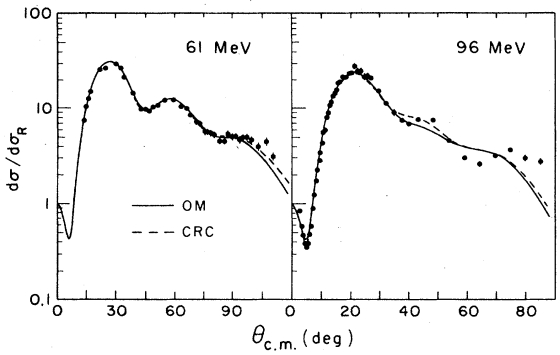

FIG. 3. Optical-model and CRC calculations of proton elastic scattering from ^{12}C, in ratio to the Rutherford cross sections.

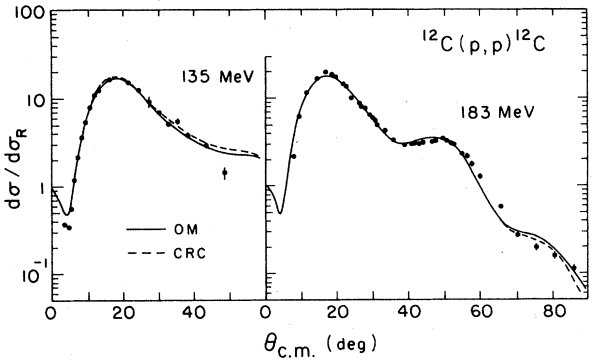

FIG. 5. Optical-model and CRC calculations of proton elastic scattering from ^{12}C, in ratio to the Rutherford cross sections.

At 40 MeV the fits in Figs. 2 and 6 are comparable to previous ones.[16] The fit to the polarization data is appreciably worse than at 21 MeV. It seems to be exceedingly difficult to obtain good fits to both cross-section and polarization data in this energy range with reasonable parameters.[41] We shall return to this point in Sec. IV. The most characteristic feature of the parameter systematics in Fig. 9 for this energy range is the rise in the spin-orbit radius to values comparable with the real central radius, and steep changes in the diffuseness parameters.

2. $E > 60$ MeV

Generally, the fits to the data were quite satisfactory in this higher-energy range and the parameters varied smoothly with energy. The fit to the 135-MeV polarization is not impressive and the χ^2 values for the cross-section data (also at 122 and 183 MeV) could be significantly reduced if the polarization data were ignored. However, there are numerous correlations among the parameters, especially between the imaginary and spin-orbit parameters, and it was difficult to establish systematic trends with only the cross-section data. The constraints of the polarization data seemed useful to have, although the experimental situation needs to be vastly improved. A recent article illustrates the value of such data at 183 MeV.[31]

Unlike Ref. 17, we had no difficulty in fitting the 61-MeV data with excellent χ^2 values and total reaction cross sections and with very reasonable parameters. Although data on reaction cross sections are scant,[30] they are useful for rejecting

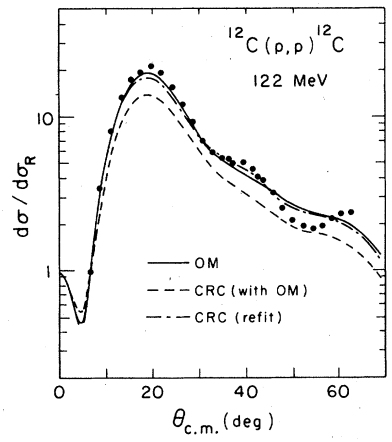

FIG. 4. Proton elastic scattering from ^{12}C at 122 MeV in ratio to the Rutherford cross sections. The solid curve is for the one-channel optical model. The dashed curve resulted from use of the same OM potential in full CRC calculations, while the dash-dot curve shows the result when the diagonal potential is adjusted for best fit to the data.

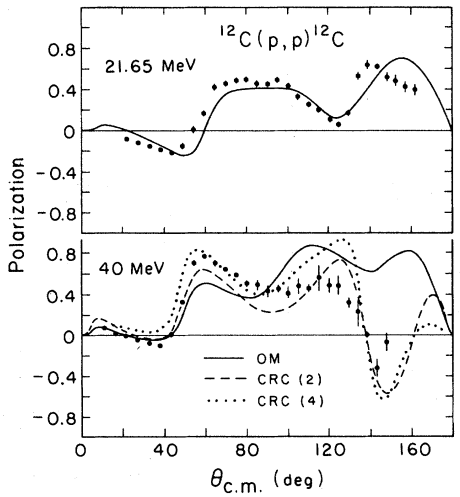

FIG. 6. The polarizations of proton elastic scattering from ^{12}C. See also the caption for Fig. 2.

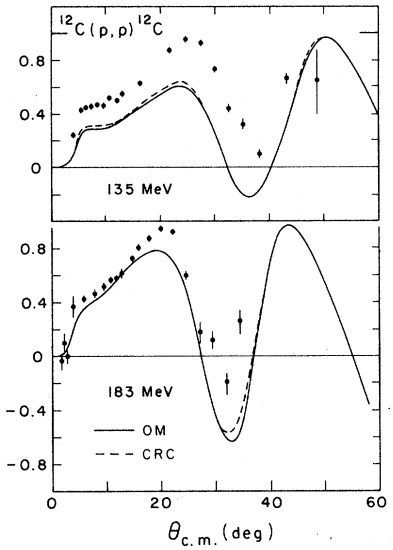

FIG. 7. The polarizations for proton elastic scattering from ^{12}C in comparison with optical-model and CRC calculations.

alternative parameter sets and trends.

The data at 96 and 122 MeV indicate more structure than is provided by the calculations in Figs. 3 and 4. The situation can be improved considerably by allowing higher-order terms due to

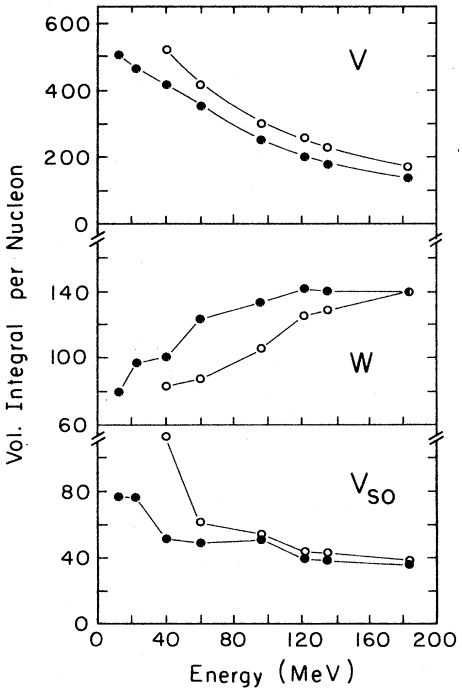

FIG. 8. Energy dependence of the volume integrals per nucleon of the real, imaginary, and spin-orbit potentials. The solid data are for the one-channel OMP and the open circles are for the ROMP of the CRC environment.

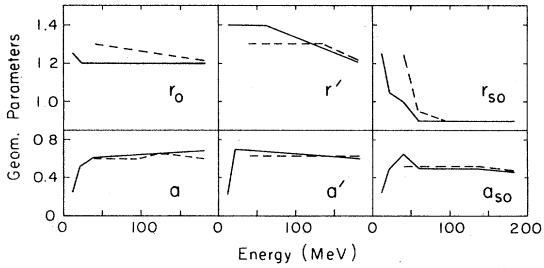

FIG. 9. Energy dependence of the geometrical parameters of the optical-model potentials. The solid lines are for the one-channel OMP and the dashed lines are for the ROMP of the CRC environment.

the permanent deformation of ^{12}C to appear in the optical potential. The radius parameter R in Eq. (4a) was replaced by $R_0[1+\beta_2 Y_2^0(\theta,\phi)]$, the resulting potential was averaged over all angles, and a search was carried out for β_2. We obtained $\beta_2 = -0.44$ with a reduction in χ^2 by a factor of 2 and with almost no change in the potential depths. The shape was improved considerably in the 30–60° range. There was little effect on the polarizations.

IV. COUPLED-CHANNEL ANALYSIS

There is little need to justify an exploration of coupled-channel effects on scattering from ^{12}C since it is well known that the strong coupling to the collective 2^+ state at 4.44 MeV is very important. In a pioneering work, Okai and Tamura demonstrated[38] that this coupling could produce resonancelike effects.

What is at stake, rather, is the number and type of channels that must be coupled. Rawitscher has shown the importance of strong couplings on both (d,p) cross sections and deuteron elastic scattering.[42] More recently, Mackintosh has investigated the effects of the coupling to pickup channels on proton scattering and reactions.[3,4,8]

The situation for ^{12}C is readily investigated. Using the CC program CHUCK2,[43] cross sections in the elastic channel were computed for pure two-step transitions proceeding through the 2^+ state of ^{12}C or the $\frac{3}{2}^-$ ground state in ^{11}C. The surprising results are shown in Fig. 10. At 135 MeV, the (p,d,p) cross sections are more than two orders of magnitude larger than the (p,p',p) cross sections. An almost identical situation holds at 180 MeV, while at 60 MeV the back coupling from the inelastic path is beginning to increase in importance. The two-step (p,d,p') cross sections to the 2^+ state (not shown) are an order of magnitude lower than the one-step yield at the first maximum, but become increasingly important at larger angles.

TABLE I. Parameters of the local, proton optical-model potential for use in one-channel calculations. The strengths have units MeV and lengths have units fm. Also listed are the total reaction cross sections (mb) and χ^2 per point for cross-section and polarization data.

E	V	r_0	a	W	r'	a'	V_{so}	r_{so}	a_{so}	σ_R	χ_σ^2/N	χ_p^2/N
12.1	−57.8	1.25	0.248	+32.6 [a]	1.40	0.223	−26.0	1.25	0.248	309	48	
21.6	−47.6	1.20	0.517	−5.76	1.40	0.70	−30.4	1.05	0.50	445	4.7	17
40	−39.3	1.20	0.61	−6.23	1.40	0.69	−21.5	1.00	0.65	343	8.8	136
61.4	−32.8	1.20	0.62	−7.54	1.40	0.67	−22.5	0.90	0.50	317	1.7	
96	−23.0	1.20	0.635	−9.00	1.35	0.655	−23.3	0.90	0.50	282	18	
122	−18.3	1.20	0.65	−10.6	1.30	0.64	−18.3	0.90	0.50	264	53	156
135	−16.2	1.20	0.66	−11.1	1.28	0.63	−17.8	0.90	0.50	252	10	114
183	−12.5	1.20	0.68	−13.1	1.20	0.61	−16.4	0.90	0.47	222	12	22

[a] Surface-derivative absorption, W is W' in Eq. (2).

It is not easy to understand the reasons for this behavior. The one-step (p,p') and (p,d) cross sections are comparable (the integrated cross sections differ by factors of 2–3). Although the cross-section ratio is also reflected in the magnitudes of the two-step transition amplitudes, those for the (p,d,p) path peak at lower l values and are more localized in l space. The (p,p') form factor peaks more than 1 fm beyond that of the (p,d) form factor. Mackintosh has given arguments regarding the significance of this.[8] Whatever the reason, the CC effects for proton scattering from ^{12}C are far more serious than had been previously thought.

This last statement does not imply that CC calculations must inevitably be done since the normal OMP might very well simulate their effects. But it is necessary to investigate this issue. Since it is impossible to incorporate all channels in detail, further effort must proceed within the framework of a model.

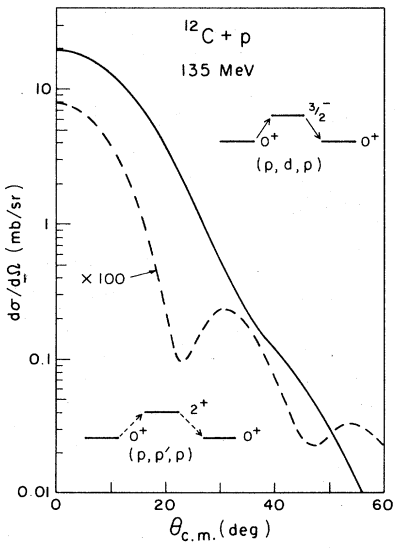

FIG. 10. Cross sections in the elastic channel of proton scattering from ^{12}C resulting from pure two-step paths for which the ground state of ^{11}C (solid curve) or the first-excited 2^+ state of ^{12}C (dashed curve) is the intermediate state.

A. CC environment

The environment we shall consider consists of proton scattering from the lowest two states of ^{12}C and (p,d) reactions to the lowest two states of ^{11}C. These states and the transfer couplings between them are shown in Fig. 11. Inelastic couplings in ^{11}C are not considered at this time.

The 2.0-MeV state of ^{11}C has almost no influence on the proton elastic cross sections, but was retained because it had a rather significant influence (destructive) on the 2^+ state of ^{12}C. A second $\frac{3}{2}^-$ level at 4.79 MeV in ^{11}C was ignored. At 122 MeV the (p,d) cross sections[23] for this state are a factor of 6 below the ground-state cross sections. The back-coupling effect on the elastic scattering is related approximately to the square of this ratio, although the influence on the 2^+ state is probably more important. It is hoped that the effects of all neglected channels are sat-

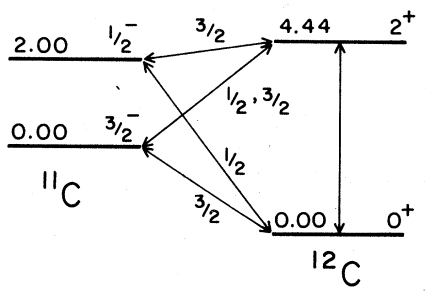

FIG. 11. The environment of the coupled-reaction-channel calculations. The states of ^{11}C and ^{12}C are labeled with their excitation energies and spin-parity values. The double-headed arrows denote two-way coupling and they are labeled also with the total angular momentum transfer j.

isfactorily taken into account in the residual ROMP.

Within this framework, which may be denoted the coupled-reaction-channel (CRC) environment,[44] the homogeneous Schrödinger Eq. (1) is replaced with a set of coupled inhomogeneous equations

$$\frac{d^2\chi_i(r)}{dr^2} + \left[k^2 - \frac{2\mu_i}{\hbar^2}U_i(r) - \frac{l(l+1)}{r^2}\right]\chi_i(r) = \sum_{j\neq i}\frac{2\mu_i}{\hbar^2}V_{ij}\chi_j(r). \quad (11)$$

Although there were only four separate mass-energy channels, angular momentum considerations resulted in as many as 15 coupled equations. These were solved exactly (infinite order) with the code CHUCK2.[43]

The off-diagonal coupling potentials $V_{ij}(r)$ for the (p,p') reaction to the 2^+ state were treated according to the collective model. The higher-order terms due to the $\beta_2 Y_2^0$ contribution to R (see Sec. III D. 2) were included, but here $\beta_2 = -0.6$ gave better agreement with experimental (p,p') cross sections. The parameters of the coupling potentials were kept equal to those of the central part of the proton ROMP during search procedures. Wave functions of Cohen and Kurath[45] were used to compute the spectroscopic amplitudes for the (p,d) reactions.

B. Deuteron potentials and form factors

A serious problem in the CRC calculations is the choice of deuteron potentials for the intermediate pickup channels. This has been discussed extensively elsewhere.[10] At first thought one might expect to use a phenomenological deuteron OMP that reproduces elastic scattering data. But if the diagonal proton OMP must be modified in a CC environment, so must also the deuteron OMP.[42] Furthermore, deuteron breakup and the general treatment of the p-n continuum are known to be very important for elastic scattering and stripping processes.[46,47] The observed failure of a conventional deuteron OMP in our calculations[10] may be related to this.

Although several detailed investigations of breakup effects have appeared in the literature,[47,48] such calculations were prohibitively large for us to incorporate. Instead we relied on the simulation provided by folded deuteron potentials. These were constructed from proton OMP's at half the deuteron energy needed in the CRC calculations. Hence, for the CRC calculations at 40, 61, 96, 122, 135, and 183 MeV, OM proton potentials were required at 12.1, 21.6, 40, 55, 61, and 80 MeV, respectively. These were determined either by direct fitting to data or from the systematics found in Sec. III. Neutron OMP's were taken to be the same as for protons.

The adiabatic model of Johnson and Soper[46] was used for this folding. Since this model contains an approximation in which the neutron and proton wave functions were treated at coincidence, it is possibly the most appropriate for our zero-range calculations. Approximate formulas for the folding have been given.[49] However, it was found sufficient merely to multiply the proton potential strengths by two (with proper adjustments for the spin-orbit portion). The Watanabe folding procedure[50] was also tried, although it may not be appropriate for simulating breakup effects. Numerical folding methods had to be adopted here. The results were sometimes sensitive to the choice of methods, an issue that will be discussed further in Sec. V.

The CRC calculations were rather insensitive to the choice of bound-state geometrical parameters, particularly with regard to the elastic scattering cross sections. The radius parameter was taken to be 1.20 fm in accordance with the proton OMP's. The diffuseness parameter varied from 0.65 fm for the Johnson-Soper calculations to 0.70 fm for those of Watanabe and the spin-orbit parameter had the conventional value $\lambda = 25$.

C. Additional factors

It is common in stripping and pickup calculations to make approximate corrections for nonlocality and finite range. These present certain theoretical difficulties in the present calculations. First of all the back feeding in the CRC calculations brings in some nonlocality directly, and secondly there are various arguments to suggest that the back feeding will be reduced considerably with an exact finite-range treatment.[51,52]

Although finite-range corrections to one-step (p,d) reactions are normally small, due to energy conservation and good well matching, off-energy-shell contributions can become very sizable in pickup-stripping processes. Coulter and Satchler indicate,[7] however, that they should be unimportant for the imaginary parts. Their effect on the real parts will be compensated in the ROMP when the elastic scattering data are refitted.

Irrespective of these difficulties, we have adopted the more conventional procedures in our model. From examination of exact finite-range calculations it was determined that calculations with nonlocality parameters $\beta = 0.85$ for protons and 0.43 for deuterons, and a finite-range parameter $R = 0.77$ (all as used in CHUCK2) gave (p,d) differential cross sections in reasonable accord with experiment at all energies.

One additional problem also could not be ex-

amined. The inclusion of both $p+^{12}C$ and $d+^{11}C$ mass partitions introduces a degree of nonorthogonality to the system. One might hope that the restriction of the model space to only the lowest two states in each partition would alleviate most of the difficulty since, physically, the different arrangements are very dissimilar and should have little overlap. It has also been argued[53] that the nonorthogonality effects are approximately canceled in pickup-stripping processes by the usual procedure of dropping the remnant terms of the interaction, thus generating a post-prior asymmetry. Explicit studies have indicated that the nonorthogonality corrections should be small.[54,55]

D. Elastic scattering results

The refitting of the elastic scattering data in the CRC environment as defined in Sec. IV. A–C was carried out with the programs CHUCK2[43] and CUPID[9] according to the iterative procedures described elsewhere.[9] Except for a partial study at 40 MeV, the calculations were limited to the energy range above 60 MeV. The most extensive searches used the Watanabe-folded deuteron potential. The results are shown in Figs. 2–7 and the parameters of the ROMP's are presented in Table II.

One might hope that this more rigorous treatment of reaction dynamics might result in improved agreement with data. In fact, the χ^2 values for both cross-section and polarization data are improved slightly, except possibly at 40 MeV. Visually the changes seem to be in the right places. However, the effects are relatively small, even for the polarization data, and we do not believe that too much significance should be attached to the improvements at this time.

The more interesting aspects are in the systematics of the parameters. Again, these systematics are partly a result of the trends that became apparent during the search procedures and partly a result of their explicit adoption. In Fig. 8 we find that the volume integral of the imaginary potential has decreased significantly at most energies, as expected. However, those for the real central and spin-orbit potentials have increased, indicating that the effects of the back couplings are repulsive.[4] It is not known whether this applies for both the (p,d,p) and (p,p') processes or what the relative energy dependence of each might be.[7]

The systematics of the geometrical parameters were also modified somewhat. There was a clear indication that, at low energies, the real radius parameters r_0 and r_{so} are significantly larger than the OM case, while the imaginary radius r' is smaller. At the high end of the energy scale the OMP and ROMP seemed to be very similar, suggesting that the CC effects were becoming less important with increasing energy.

An important consideration here is the degree to which optical-model parameters might simulate the effects of channel couplings and whether the "bare" potential might be distorted thereby. Answers are very difficult to obtain, in large part because of cross correlations between various parzmeter groups. Nevertheless, there may very well be substantial effects, especially on radius parameters at low energies and particularly for r_{so}.

E. The 40-MeV case

The calculations at 40 MeV gave a special problem. Unlike the situation at higher energies, where the search procedures converged after two

TABLE II. Parameters of the proton residual optical-model potential for use in the CRC environment described in Sec. IV. See also the caption of Table I.

E	V	r_0	a	W	r'	a'	V_{so}	r_{so}	a_{so}	σ_r	χ_σ^2/N	χ_p^2/N
Watanabe-folded deuteron potential												
40	−40.8	1.30	0.60	−6.14	1.30	0.63	−37.8	1.25	0.52	395	34	75
61.4	−33.7	1.29	0.57	−6.56	1.30	0.63	−27.1	0.95	0.52	299	1.0	
96	−24.8	1.275	0.60	−8.00	1.30	0.63	−25.1	0.90	0.52	261	14	
122	−20.9	1.26	0.65	−9.47	1.30	0.63	−19.3	0.90	0.52	261	55	119
135	−18.9	1.25	0.65	−9.69	1.30	0.63	−19.9	0.90	0.52	252	8	91
183	−15.2	1.23	0.60	−11.6	1.23	0.63	−17.2	0.90	0.48	227	11	21
Johnson-Soper folded deuteron												
61.4	−32.6	1.29	0.60	−6.06	1.30	0.63	−25.0	0.95	0.52	281	1.2	
96	−24.5	1.275	0.60	−8.00	1.30	0.63	−25.1	0.90	0.52	263	15	
122	−20.9	1.26	0.65	−9.49	1.30	0.63	−19.0	0.90	0.52	260	49	120
135	−19.2	1.25	0.65	−9.47	1.30	0.63	−19.2	0.90	0.52	248	6	95
183	−15.4	1.23	0.60	−11.8	1.30	0.63	−16.8	0.90	0.48	230	10	22

or three iterations, the cycle between successive CHUCK2 and CUPID calculations seemed unstable. The best results from the optical-model search program were obtained with the ROMP in Table II used in conjunction with the back couplings from the second iteration through CHUCK2. The χ^2 for the cross sections was about the same as for the OM parameters of Table I, while that for the polarization data was very substantially improved.

Unfortunately, what initially seemed like a convergent process became a slightly divergent one. After four iterations the parameters of the ROMP had settled down to fairly stable values, but the χ^2 values had increased significantly, particularly for the cross sections. The results of both iterations are shown in Figs. 2 and 6 and in Table II.

The main difficulty seemed to be at back angles. The back-coupling amplitudes had a strong tendency to put a sharp rise in the elastic cross sections beyond 140° and changes in the geometrical parameters of the ROMP were necessary to bring it back down. The most significant changes were a sharpening of the edge of the spin-orbit potential and its shift to larger radii.

In spite of the difficulties, one conclusion seems clear. The CRC environment has resulted in very substantial improvement of the fit to the polarization data, with not much change in the fit to the cross-section data. Qualitatively, the ratio of the polarizations at the 60° and 120° humps has been nearly inverted and a dip near 140° has been formed, which is in much better agreement with the experimental patterns. Satchler has reported much difficulty in fitting simultaneously both cross-section and polarization data in this energy range.[41] We suggest that the problems may be intimately associated with the influence of strongly coupled pickup channels. The difficulties with the convergence here are possibly related to ambiguities regarding calculational procedures, some of which are discussed in the next section.

V. DWBA or CRC?

Although there was a general and systematic improvement in χ^2 values in the CRC environment, this was not very large. This suggests that, at intermediate energies, the local, complex OMP might be doing an excellent job of representing all the complications of proton elastic scattering from ^{12}C. The question naturally arises whether this simulation ability also extends to proton-induced reactions.

It should be understood that this favorable state of affairs is not a consequence of very small back-coupling amplitudes. This is made clear in Fig. 4 where the dashed curve represents the elastic scattering cross section in the full CRC environment, but with the normal OMP from Table I used for the proton channels. The cross section has dropped by up to 30–40% compared with the pure one-channel OM result. It is only when the proton potential is replaced with the ROMP from Table II that the CRC calculations give the proper result.

The situation for reactions is very similar. This is illustrated in Fig. 12 for the (p,p') reaction to the lowest 2^+ state in ^{12}C and the (p,d) reaction to the ground state of ^{11}C, both at 122 MeV. The solid lines are the results of conventional DWBA calculations (pure one-way transitions from the ^{12}C ground state to the final states). When the one-channel proton OMP is used in the CRC calculations there is again a decrease in the cross sections, although this is not very large for the (p,d) reaction. After the elastic scattering data had been refitted, the final CRC results at the first maxima were very much like the original DWBA calculations. For the 2^+ state, however, there is some enhancement at large angles, a result anticipated in the exploratory calculation of Sec. IV. (The failure to reproduce the data very well beyond the first maximum is believed to be due primarily to the neglect of the deformed spin-orbit coupling interaction.[2])

This pattern of behavior was similar for both choices of folded deuteron potentials and there was little distinction between the choices at the higher energies. The (p,p') cross sections were insensitive to this, even at the lower energies. However, as illustrated in Fig. 13, the (p,d) ground-state cross sections were distinctively different for the Johnson-Soper or Watanabe po-

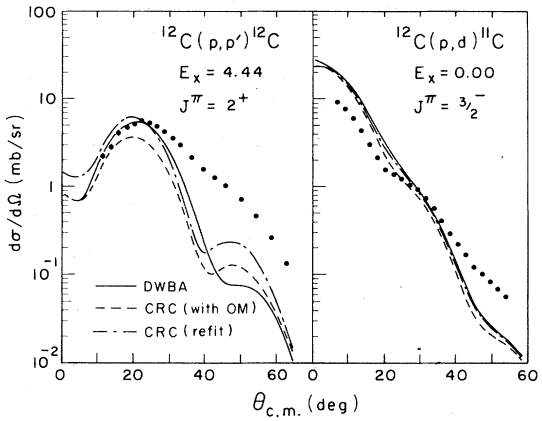

FIG. 12. Calculations of cross sections for the (p,p') reaction to the lowest 2^+ state of ^{12}C and the (p,d) reaction to the ^{11}C ground state, in comparison with data at 122 MeV. See also the caption for Fig. 4.

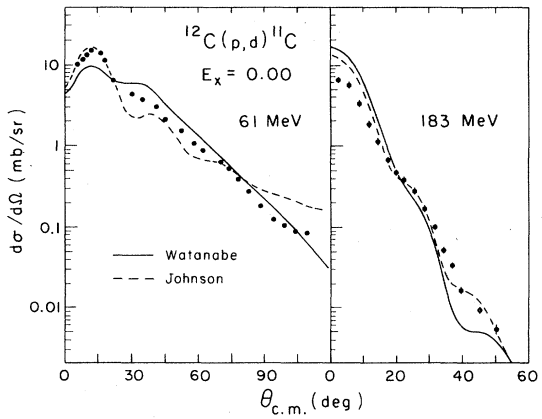

FIG. 13. Calculations of (p,d) cross sections to the ^{11}C ground state at two energies in comparison with data. The solid curve represents use of the Watanabe-folded deuteron potential, while the dashed curve corresponds to Johnson-Soper folding.

tentials. There is some preference for the results with the Johnson-Soper adiabatic potential (even a slight preference at 183 MeV). However, it seems that the (p,d) calculations do not exactly fit the slope of the data at any energy. Certainly the choice of deuteron potential is a very important consideration, but it is difficult at this time to reach specific conclusions regarding it.

A possible consideration here is the effects of inelastic excitations in ^{11}C. The Cohen-Kurath wave functions[45] predict that there should be many important couplings between the states of ^{11}C and that $\Delta J = 1$ transitions ($\Delta L = 0$ and 2, $\Delta S = 1$) may be quite important. Unfortunately, these will increase the complexity of the CRC calculations very substantially. Macroscopically, the $\Delta L = 2$ parts might be handled (along with $\Delta J = 2$ transitions) with the usual collective model, but the $\Delta L = 0$ terms are also likely to be significant at intermediate energies. Microscopically, the spin-flip portions of the isoscalar excitations may not be well described.[2]

A test calculation at 122 MeV with a single inelastic coupling in ^{11}C indicated that the ground-state (p,d) cross sections could be reduced slightly at forward angles, in better agreement with the data. Although the CRC environment is now different from that in Sec. IV, it is unlikely that this improvement would be eliminated completely when the proton ROMP is readjusted since the influence on the elastic channel is of higher order.

Thus, although the DWBA calculations seem to be entirely adequate for describing the main features of the transitions, many details also seem to depend on the singular effects brought about by individual channel couplings. Since the full apparatus of CRC calculations makes very large demands on computer resources, one might hope that certain approximations would allow these singular features to be described with sufficient accuracy. Calculations of two-step contributions (second-order DWBA) has been a common approach and this has the advantage that the amplitudes from several paths leading to the same final state may be calculated separately and added together.

In testing this approach, calculations were made of the 122-MeV pickup-stripping (p,d,p') cross sections to the 1^+ states of ^{12}C at 12.71 and 15.11 MeV. In the first approach the full CRC environment of Fig. 11 was used, but with one-way transitions from both ^{11}C states to the 1^+ states of ^{12}C also included. The ROMP from Table II was used for all proton channels. In the second approach only the one-way transitions from the ^{12}C ground state to both ^{11}C states were specified, followed by the same one-way transitions up to the 1^+ states. The OMP from Table I was used for all proton channels here. The cross sections for the 1^+ states from both approaches were identical out to about 30°, while the pure two-step cross sections were slightly lower at larger angles.

It should be noted that three-step contributions from paths that proceed through the 2^+ state of ^{12}C were not included in the second approach. They are expected to be relatively small, particularly at forward angles. Furthermore, no distinctions have been made between the OM potentials of the entrance and exit channels.[56] The calculations here seem to work best when these are the same, but the issue needs more exploration.

The most important result of the investigation in this section is that the particular effects of the CRC environment appear to decrease with energy. Not only was the convergence of the iterated search procedures better, but the differences between the ROMP and OMP decreased and the results were also less sensitive to uncertainties regarding details, such as the choice of deuteron potentials. Thus, it appears that the DWBA methods become more suitable as the energy increases and that the complexities of the CRC calculations are less necessary.

This result is of course reflected in the magnitudes of the back-coupling amplitudes in the elastic channel. A way to express this is illustrated in Fig. 14. For three energies we have plotted the ratios of the S-matrix elements $S_{ij} = \exp(2i\delta_{dj})$ obtained from the ROMP's of Table II and OMP's of Table I and also the changes in the nuclear

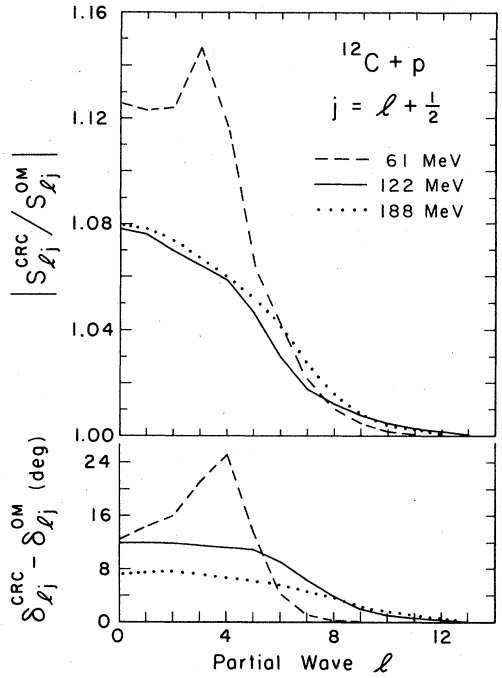

FIG. 14. Ratios of the amplitudes of the S-matrix elements and the differences in phase for the OMP's and ROMP's from Tables I and II at three energies.

phase shifts δ_{lj}. As the energy increases, the ratios of the S-matrix elements and the differences in phase shifts tend to decrease. The principal effects are in the lowest partial waves where the S-matrix amplitudes of the ROMP are several percent larger and are shifted in phase to larger angles. For the partial waves with $j = l - \frac{1}{2}$, the ratios of S-matrix amplitudes are essentially the same as those shown in Fig. 14. The changes in the phases are a little smaller at 183 MeV, but considerably smaller at 61 MeV.

The behavior of the ratios and shifts is smooth at the higher energies, but shows some irregularities at 61 MeV. The situation is reminiscent of patterns found in the scattering of protons from ^{16}O and ^{40}Ca, where phenomenological l-dependent potentials were included in the analysis.[57,58] The l-dependent effects were similarly concentrated in the lowest partial waves and it was suggested that the phenomenological l dependence was related to couplings to pickup channels.[58,59] Additional explorations of this question would be interesting.

VI. DISCUSSION AND CONCLUSIONS

The phenomenological analysis of proton scattering from ^{12}C in both the optical-model and coupled-channel approaches has revealed numerous systematic features. It has also shown clearly that ^{12}C is quite suitable for the study of nuclear reactions and scattering and that calculations for these processes can be reliable. The situation is best at intermediate energies, say $E > 100$ MeV, and seems adequate for energies as low as about 60 MeV. Below that the effects of strong couplings to other channels become particularly important in a manner that requires attention to all details.

This dichotomy about an energy near 60 MeV is revealed in many ways. The volume integrals and geometrical parameters shown in Figs. 8 and 9 seem to have smooth and regular trends above that energy. The trends are distinctively different below 60 MeV, particularly for the spin-orbit geometrical parameters and the other diffuseness parameters. At the higher energies the effects of the back couplings are not very substantial, while at lower energies they can have a dramatic impact on cross sections and polarizations. This was becoming apparent in the analysis of the 61-MeV data, where the (p, d) angular distributions showed greater sensitivity to the choice of the deuteron optical-model potential. At 40 MeV the effects were quite severe. Undoubtedly the calculations here are being hurt by the approximations used: the zero-range assumption, the neglect of nonorthogonality corrections, and the incomplete treatment of deuteron breakup and the p-n continuum.

An important conclusion here is that the local, complex OMP is able to simulate the effects of channel couplings quite well in many instances, a feature that improves with increasing energy. Furthermore, the use of this OMP in DWBA calculations of reactions appears to be realistic and justified even from a more detailed approach. The important criterion is that the elastic scattering data should be reproduced well. Some features of a more encompassing CRC model may yet remain to be included, but it appears feasible to evaluate these by use of the second-order DWBA.

It must be stressed that this study has focused attention almost exclusively on transitions that have large spectroscopic couplings with the elastic channel. In terms of past experience one expects these to be primarily single-step processes. Transitions that are inhibited in terms of direct couplings, such as the excitation of the 4^+ state of ^{12}C, will still require appropriate treatment of multistep contributions. Second-order DWBA may be adequate for some of these, while the full CRC environment may be needed for others. The CRC may also be necessary for details of the uninhibited transitions.

One may thus conclude that the DWBA calculations of the $^{12}C(p, p')^{12}C$ reaction at 122 MeV

in the preceding article[2] are entirely adequate. This has much significance since the contributions from knockon exchange are very considerable and no codes exist which can calculate them exactly in the CRC model described in Sec. IV. Thus, the focus of Ref. 2 was properly directed towards the microscopic effective interaction. Although some effects from two-step processes may be present, as was discussed in Ref. 2, the treatment of the reaction dynamics is not a serious limitation on the conclusions.

There are no major surprises in the conclusions expressed so far. Indeed they are implicit in much of current practice. More explicitly they may be considered to be an extension into the CRC environment of the tendency to equivalence between DWBA and CC calculations previously noted[60] for strong inelastic couplings, under the constraint that elastic scattering data be fit equally well. Nevertheless, it is gratifying to have them emerge directly front the phenomenological analyses in the present study.

Again the reader is cautioned that the favorable state of affairs expressed here does not extend to lower energies, such as below 60 MeV. As the back-coupling amplitudes take on greater importance (e.g., as the inelastic coupling parameter β increases),[60] the equivalence between DWBA and coupled-channel approaches breaks down. Although resonances of various types may produce significant effects at the lower energies,[38,39,61] we concur with Mackintosh that couplings to pick-up channels are probably the most important ones for light nuclei. Similar conclusions were also reached for low-energy nucleon scattering from molybdenum isotopes.[62]

Unfortunately, one item of considerable interest could not be illuminated very clearly in the present work. The strengths and geometrical parameters of one-channel OMP's resulting from phenomenological analyses of elastic scattering data are often used to infer features of microscopic effective interactions and geometrical properties of nuclei. It is important to determine the extent to which these parameters have become distorted from their more intrinsic values in order to compensate for and to simulate channel-coupling effects. The sharp decrease in the diffuseness parameters at low energies in Fig. 9 is surely an indication of this. However, in view of the difficulties even at 40 MeV it became impractical to extend the analysis to these low energies.

The cross correlations between parameter groups also precluded specific conclusions from being drawn regarding such simulation effects. While it is difficult to make general statements, there appeared to be various compensations between the parameters of the imaginary and the spin-orbit potentials. Furthermore, the differences of the proton OMP's and ROMP's, as discussed in Sec. V, are asymmetric with respect to the spin-orbit components of the partial waves. What implications this may have for phenomenological imaginary spin-orbit potentials is not clear since the data considered here were not especially sensitive to them.

It is felt that greater insight into the issues raised here would come if the experimental situation were improved. A well-designed program of the elastic scattering of nucleons and other light projectiles at intermediate energies from several targets would be beneficial. It is especially important that cross-section and polarization data span large angular ranges and that data for the predominant reactions also be available. The energies should span a range such that back-coupling effects are significant at one end and relatively unimportant at the other. It is not known how this energy range depends on mass number. As the mass increases, the averaging effects of more open channels should probably keep the range from being higher than that considered for ^{12}C here.

Finally, although substantial and excellent progress has been made in recent years in terms of theoretical techniques, some difficult problems remain to be examined in more detail. Probably the most important for the type of analyses discussed here is the handling of the intermediate channels. Since large-scale CRC calculations are impractical and simple adiabatic potentials[46] may be inadequate,[48] realistic approximation techniques need to be devised. In combination with new experimental data, these techniques may reasonably be expected to lead to great enrichment in our understanding of effective nucleon-nucleus interactions.

ACKNOWLEDGMENTS

This work was supported in part by the National Science Foundation. Many of the computer calculations were also carried out with internal support. We also gratefully acknowledge many fruitful discussions on all aspects of this work with Dr. C. M. Vincent.

[1]R. E. Anderson, J. J. Kraushaar, J. R. Shepard, and J. R. Comfort, Nucl. Phys. A311, 93 (1978).
[2]J. R. Comfort, S. M. Austin, P. T. Debevec, G. L. Moake, R. W. Finlay, and W. G. Love, Phys. Rev. C 21, 2147 (1980), preceding paper.
[3]R. S. Mackintosh, Nucl. Phys. A164, 398 (1971).
[4]R. S. Mackintosh and A. M. Kobos, Phys. Lett. 62B, 127 (1976).
[5]J. P. Jeukenne, A. Lejeune, and C. Mahaux, Phys. Rep. 25C, 83 (1976); Phys. Rev. C 16, 80 (1977).
[6]F. A. Brieva and J. R. Rook, Nucl. Phys. A291, 299 (1977); A291, 317 (1977); A297, 206 (1978); A307, 493 (1978).
[7]P. W. Coulter and G. R. Satchler, Nucl. Phys. A293, 269 (1977).
[8]R. S. Mackintosh, Nucl. Phys. A209, 91 (1973); A230, 195 (1974).
[9]J. R. Comfort, Comput. Phys. Commun. 16, 35 (1978).
[10]J. R. Comfort and B. C. Karp, Phys. Lett. 80B, 1 (1978).
[11]J. R. Comfort, in *Proceedings of INS International Symposium on Nuclear Direct Reaction Mechanisms, Fukuoka, Japan, 1978,* edited by M. Tanifuji and K. Yazaki (INS, University of Tokyo, 1978), p. 118.
[12]J. R. Comfort in *Proceedings of the Conference on (p,n) Reactions and the Nucleon-Nucleon Force, Telluride, Colorado, 1979,* edited by C. D. Goodman, S. M. Austin, S. T. Bloom, J. R. Ropaport, and G. R. Satchler (Plenum, New York, 1980), p. 303.
[13]Y. Nagahara, J. Phys. Soc. Jpn. 16, 133 (1961).
[14]J. K. Dickens, D. A. Haner, and C. N. Waddell, Phys. Rev. 132, 2159 (1963).
[15]R. M. Craig, J. C. Dore, G. W. Greenlees, J. Lowe, and D. L. Watson, Nucl. Phys. 79, 177 (1966).
[16]L. N. Blumberg, E. E. Gross, A. van der Woude, A. Zucker, and R. H. Bassel, Phys. Rev. 147, 812 (1966).
[17]C. B. Fulmer, J. B. Ball, A. Scott, and M. L. Whiten, Phys. Rev. 181, 1565 (1969).
[18]P. G. Roos, S. M. Smith, V. K. C. Cheng, G. Tibell, A. A. Cowley, and R. A. J. Riddle, Nucl. Phys. A255, 187 (1975).
[19]G. Gerstein, J. Niederer, and K. Strauch, Phys. Rev. 108, 427 (1957). Data are tabulated by H. J. Kim, W. T. Milner, and F. K. McGowan, Nucl. Data A2, 1 (1966).
[20]J. M. Dickson and D. C. Salter, Nuovo Cimento 6, 235 (1957).
[21]S. K. Mark, P. M. Portner, and R. B. Moore, Can. J. Phys. 44, 2961 (1966).
[22]J. R. Comfort, G. Moake, C. Foster, J. Rapaport, and C. Goodman, Bull. Am. Phys. Soc. 24, 829 (1979).
[23]R. E. Anderson, J. R. Shepard, and J. R. Comfort, Bull. Am. Phys. Soc. 21, 979 (1976).
[24]O. N. Jarvis, M. Shah, and C. Whitehead, Harwell Report No. AERE-R6769, 1971 (unpublished).
[25]J. McL. Emmerson, J. C. W. Madden, C. M. P. Johnson, N. Middlemas, A. B. Clegg, and W. S. C. Williams, Nucl. Phys. 77, 305 (1966).
[26]C. Rolland, B. Geoffrion, N. Marty, M. Morlet, B. Tatischeff, and A. Willis, Nucl. Phys. 80, 625 (1966).
[27]V. Comparat, R. Frascaria, N. Marty, M. Morlet, and A. Willis, Nucl. Phys. A221, 403 (1974).
[28]R. Alphonce, A. Johansson, and G. Tibell, Nucl. Phys. 4, 672 (1957).
[29]A. Johansson, U. Svanberg, and P. E. Hodgson, Ark. Fys. 19, 541 (1961).
[30]A. Johansson, U. Svanberg, and O. Sundberg, Ark. Fys. 19, 527 (1961).
[31]A. Ingemarsson, O. Jonsson, and A. Hallgren, Nucl. Phys. A319, 377 (1979).
[32]D. Hasselgren, P. U. Renberg, O. Sundberg, and G. Tibell, Nucl. Phys. 69, 81 (1965).
[33]J. Källne and E. Hagberg, Phys. Scr. 4, 151 (1971).
[34]W. S. C. Williams, *An Introduction to Elementary Particles* (Academic, New York, 1961), Appen. A.
[35]M. Goldberger and K. M. Watson, *Collision Theory* (Wiley, New York, 1964), Sec. 6.8.
[36]F. D. Becchetti, Jr., and G. W. Greenlees, Phys. Rev. 182, 1190 (1969).
[37]J. S. Nodvik, C. B. Duke, and M. A. Melkanoff, Phys. Rev. 125, 975 (1962).
[38]S. Okai and T. Tamura, Nucl. Phys. 31, 185 (1962).
[39]T. Tamura and T. Terasawa, Phys. Lett. 8, 41 (1964).
[40]J. J. Kolata and A. Galonsky, Phys. Rev. 182, 1073 (1969).
[41]G. R. Satchler, Nucl. Phys. A100, 497 (1967).
[42]G. H. Rawitscher, Phys. Rev. 163, 1223 (1967).
[43]P. D. Kunz (unpublished); extended version of J. Comfort.
[44]W. R. Coker, T. Udagawa, and H. H. Wolter, Phys. Rev. C 7, 1154 (1973).
[45]S. Cohen and D. Kurath, Nucl. Phys. 73, 1 (1965).
[46]R. C. Johnson and P. J. R. Soper, Phys. Rev. C 1, 976 (1970).
[47]G. H. Rawitscher, Phys. Rev. C 9, 2210 (1974); 11, 1152 (1975).
[48]J. P. Farrell, C. M. Vincent, and N. Austern, Ann. Phys. (N.Y.) 96, 333 (1976); 114, 93 (1978).
[49]G. L. Wales and R. C. Johnson, Nucl. Phys. A274, 168 (1976).
[50]S. Watanabe, Nucl. Phys. 8, 484 (1958).
[51]P. D. Kunz and L. A. Charlton, Phys. Lett. 61B, 1 (1976).
[52]P. D. Kunz, in Ref. 12.
[53]T. Udagawa, H. H. Wolter, and W. R. Coker, Phys. Rev. Lett. 31, 1507 (1973).
[54]S. R. Cotanch and C. M. Vincent, Phys. Rev. Lett. 36, 21 (1976).
[55]S. R. Cotanch and C. M. Vincent, Phys. Rev. C 14, 1739 (1976).
[56]R. J. Ascuitto, J. F. Petersen, and E. A. Seglie, Phys. Rev. Lett. 41, 1159 (1978).
[57]A. M. Kobos and R. S. Mackintosh, J. Phys. G 5, 97 (1979).
[58]R. S. Mackintosh and A. M. Kobos, J. Phys. G 5, 359 (1979).
[59]R. S. Mackintosh and L. A. Cordero-L., Phys. Lett. 68B, 213 (1977).
[60]F. Perey and G. R. Satchler, Phys. Lett. 5, 212 (1963).
[61]K. A. Amos, H. V. Geramb, R. Sprickmann, J. Arvieux, M. Buenerd, and G. Perrin, Phys. Lett. 52B, 138 (1974).
[62]J. R. Comfort, Phys. Rev. Lett. 42, 30 (1979).